

# Environmental factors affecting regional differences and decadal variations in the buried flux of marine organic carbon in eastern shelf sea areas of China

Qian Yang<sup>1,2</sup>, Keming Qu<sup>1,2,3</sup>, Shu Yang<sup>1,2</sup>, Yao Sun<sup>1,2\*</sup>, Yan Zhang<sup>1,2</sup>, Mingying Zhou<sup>1,2</sup>

<sup>1</sup>Yellow Sea Fisheries Research Institute, Chinese Fisheries Science Academy, Qingdao 266071, China

<sup>2</sup>Key Laboratory of Sustainable Development of Marine Fisheries, Ministry of Agriculture, Qingdao 266071, China

<sup>3</sup>Key Laboratory of Aquatic Product Processing, Ministry of Agriculture and Rural Affairs, Chinese Academy of Fishery Sciences, Beijing 100141, China

Received 28 October 2019; accepted 13 January 2020

© Chinese Society for Oceanography and Springer-Verlag GmbH Germany, part of Springer Nature 2021

## Abstract

To characterize environmental factors controlling decadal-scale variations in the buried flux of marine organic carbon ( $BF_{C_m}$ ) in the eastern shelf sea areas of China (ECSS), four well preserved sediment cores collected from the central Yellow Sea mud (CYSM) area, the Yellow Sea Coastal Current (YSCC) area and the Changjiang River Estuary (CRE) were investigated in this study. In the CYSM, variations in  $BF_{C_m}$  were found to be dependent on variations in primary productivity and to exhibit a cyclical trend possibly related to fluctuations in the Pacific Decadal Oscillation (PDO) and the East Asian winter monsoon index (EAWM). In the YSCC,  $BF_{C_m}$  likewise depends on primary productivity. Prior to the 1950s, variations in  $BF_{C_m}$  were similar to that of the EAWM. After the 1950s,  $BF_{C_m}$  increased rapidly and exhibited maximum values in the surface layer, consistent with an increase in primary productivity caused by the input of terrestrial nutrients associated with China's economic development. In the CRE, variations in  $BF_{C_m}$  were affected by several competing factors making it difficult to identify clear relationships between variations in  $BF_{C_m}$  and primary productivity. In contrast, long-term variability in  $BF_{C_m}$  is more similar to changes in the Changjiang River sediment load. Thus, it is speculated that the construction of dams along the Changjiang River may be the main cause of variations in  $BF_{C_m}$  in this area. Given the disproportionate effects of human activities on marine environments and decadal variations in  $BF_{C_m}$  in the ECSS, careful attention should be paid to regional differences in organic carbon preservation and environmental changes lest estimates of these values be made imprecise or inaccurate.

**Key words:** marine organic carbon, buried flux, primary productivity, climate change, human activity

**Citation:** Yang Qian, Qu Keming, Yang Shu, Sun Yao, Zhang Yan, Zhou Mingying. 2021. Environmental factors affecting regional differences and decadal variations in the buried flux of marine organic carbon in eastern shelf sea areas of China. *Acta Oceanologica Sinica*, 40(6): 26–34, doi: 10.1007/s13131-020-1601-5

## 1 Introduction

Biological carbon sequestration on continental shelves is mainly achieved through primary productivity and burial of marine organic carbon. Under the right circumstances, a large fraction of marine organic carbon can settle and be buried in sediment, leading to long-term removal of this carbon from the marine carbon cycle. Thus, burial of carbon in marine sediments is considered a long-term reservoir for atmospheric  $CO_2$ .

The South Yellow Sea (SYS) and the East China Sea (ECS) are important shelf seas off the coast of China. Recently, several studies have addressed various aspects of the sinks/sources of carbon burial in the continental shelf. For example, previous studies revealed that organic carbon buried in marine sediments primarily represent fluvial and marine sources. Notably, marine organic carbon derived from marine primary productivity is generally recognized as an important indicator of the potential for marine

carbon sequestration. Several studies have demonstrated that the C/N ratio,  $\delta^{13}C$  and phytoplankton biomarkers may be used as effective proxies for tracing marine organic carbon (Cai et al., 2014; Lin et al., 2014; Wu et al., 2016). To better evaluate the potential effects of natural processes and anthropogenic activities on coastal carbon sinks, chronological data were used to reconstruct the evolution of marine-derived organic carbon ( $C_m$ ) storage in shelf sediments (Zhang et al., 2017). Li et al. (2015) analyzed the historical trend of total organic carbon burial in the CRE and determined that the proportion of organic carbon from terrigenous ( $C_t$ ) buried in sediment is higher than  $C_m$ . These authors considered that the sedimentary record of the CRE can reflect the influence of human activities on the natural environment. Yang et al. (2011) analyzed the burial of organic carbon in the Holocene sediments of the Zhujiang River and the CRE, and found that the historical record of organic carbon in the Zhuji-

Foundation item: The Fund of Key Laboratory of Control of Quality and Safety for Aquatic Products, Ministry of Agriculture and Rural Affairs, P. R. China under contract No. 2021C001; the National Key Research and Development Program of China under contract No. 2018YFD0900703; the Major Scientific and Technological Innovation Project of Shandong Provincial Key Research and Development Program under contract No. 2019JZZY020706.

\*Corresponding author, E-mail: sunyao@yafri.ac.cn

ang River Estuary is closely related to the evolution of the East Asian winter monsoon index (EAWM), while the burial of organic carbon in the CRE is affected by many factors and exhibits no correlation with monsoon cycles. Cai et al. (2014) reconstructed sedimentary records of organic carbon in the ECS and the Yellow Sea and found that trends in  $C_m$  over the past 200 a were consistent with changes in sea surface temperature and primary productivity. Additionally, Hu et al. (2016) pointed out that the storage capacity of organic carbon in the Bohai Sea and the Yellow Sea is dominated by the fluvial input of land-based organic matter, high level of phytoplankton primary productivity, convergent hydrodynamic and stable depositional settings. The above studies indicate that there may be regional and temporal variations in the burial rate and eventual fate of organic carbon that have occurred over the last 100 a. However, these variations and the factors that influence them have not been systematically studied at the inter-regional scale. If the regional differences are common along the shelf as predicted, the conclusions of previous studies on relationships between marine organic carbon storage capacity and environment variations may be imprecise, as such regional differences are typically ignored or else poorly quantified.

In this study, four well preserved sediment cores collected in different regions of the eastern shelf sea areas of China (ECSS) are analyzed for  $^{210}\text{Pb}$  isotopes and total organic carbon/total nitrogen (TOC/TN) ratios to reconstruct the historical records of the sources of modern organic matter (OM) and the related composition of  $C_m$ . Moreover, to assess regional differences in marine-derived carbon sequestration and the effects of natural processes and human activities on the buried marine organic carbon flux ( $\text{BF}_{C_m}$ ) in different areas,  $\text{BF}_{C_m}$  in the SYS, ECS, and CRE was calculated.

## 2 Methods

### 2.1 Sample collection

The SYS and ECS are typical marginal seas of the Northwest Pacific Ocean. The coastal current in the SYS and the ECS mainly include the Yellow Sea Coastal Current (YSCC), the Yellow Sea Warm Current (YSWC) and the West Korean Coastal Current (WKCC). Sediments in these areas are primarily influenced by the supply of terrestrial sources from the Huanghe River and the Changjiang River. To the southeast, these sea areas mainly exhibit oceanic characteristics because of the effects of the YSWC, which is an offshoot of the Kuroshio Current. In contrast, the northeast and western regions are more greatly affected by the adjacent terrestrial environment and the YSCC. In this study, decadal variations in marine-derived carbon sequestration are determined based on four sediment cores collected from the ECSS in April 2006 and June 2009 (Fig. 1). Station B19, near the 50 m isobath off the southwestern coast of the Shandong Peninsula, is significantly affected by the YSCC. Stations A7 and B14 in the central Yellow Sea mud (CYSM) area are significantly affected by the YSWC. Station H1-18 is located in the transitional zone between the Changjiang River Delta and the shelf sea, and is significantly affected by input of terrigenous source material from the nearby the Changjiang River Estuary (CRE).

Sediment cores were collected using a box sampler and then stored at  $-4^\circ\text{C}$  prior to being cut in the laboratory. Subsamples were achieved at 1 cm intervals in the upper 15 cm of the core, and at 2 cm intervals for the rest of the core. After drying to a constant weight at  $60^\circ\text{C}$ , the sediments were analyzed. All samples in Core A7 and Core B14 are characterized by silty clay, while sedi-

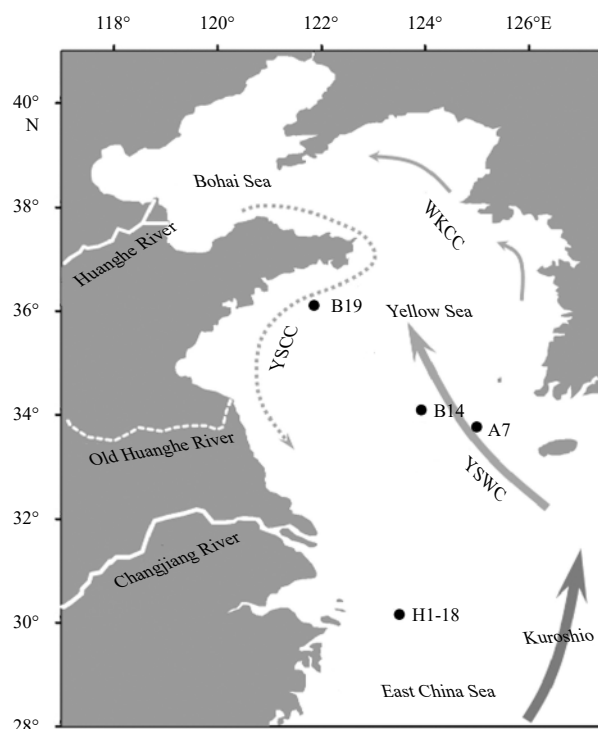


Fig. 1. Sampling stations of Cores B19, B14, A7, and H1-18. YSCC: the Yellow Sea Coastal Current; YSWC: the Yellow Sea Warm Current; WKCC: the West Korean Coastal Current.

ments in Core B19 and Core H1-18 were composed of clay and clayey sand, respectively.

### 2.2 $^{210}\text{Pb}$ analysis

The activities of  $^{210}\text{Pb}_{\text{ex}}$  and  $^{226}\text{Ra}$  in cores were determined using a germanium detector manufactured by AMETEK Company at the Institute of Polar Environment, University of Science and Technology of China.  $^{210}\text{Pb}$ -derived sediment accumulation rates (SARs) were calculated based on the constant initial concentration (CIC) model.

### 2.3 Measurement of total carbon (TC), TOC and TN

Original samples were dried to constant weight at  $60^\circ\text{C}$ . After being ground in an electric grinding mill and sieved through a 60-mesh sieve, TC was measured by element analyzer (Elementar vario ELIII, Langensfeld, Germany) with an analytical precision of 0.1%. Repeat measurement errors of TC are less than 1%. Approximately 1.5 g of freeze-dried samples was fumigated with hydrochloric acid for 24 h to remove inorganic carbon. TOC and TN values were then determined using the elemental analyzer.

### 2.4 Estimation of $C_m$

The C/N ratio has been previously identified as a valuable indicator of sedimentary organic matter sources. Terrestrial organic matter is generally characterized by ratios of  $\text{C/N} > 12$ . Sedimentary organic matter is thought to be marine autogenic if the ratio of C/N is below 8 (Meyers, 1994; Dean, 1999). The C/N ratio has been widely used to evaluate the relative contributions of terrestrial and marine autogenic sources (Perdue and Koprivnjak, 2007; Chen et al., 2011). Previous studies have suggested that the terrestrial and marine end-member values of C/N are typically 5 and 20, respectively (Jia et al., 2002; Li et al., 2008). For this study,  $C_m$  was calculated based on the formula presented by Qian et al. (1997) as follows:

$$\text{TOC} = C_m + C_t, \quad (1)$$

$$\text{TN} = N_a + N_t, \quad (2)$$

$$N_m = C_m/5, \quad (3)$$

$$N_t = C_t/20, \quad (4)$$

where TOC and TN are the measured TOC and TN, respectively;  $C_m$  and  $N_m$  are the marine-derived organic carbon and nitrogen contents, respectively;  $C_t$  and  $N_t$  are the contents of organic carbon and nitrogen from terrigenous inputs, respectively. From the above equations, the following equation can be derived:

$$C_m = (20\text{TN} - \text{TOC})/3. \quad (5)$$

### 2.5 Organic matter provenance

A binary mixing model was developed to quantitatively estimate the contribution of OM in the studied cores, based on the principle of a conservative mixture of different end-member values of C/N and the law of mass conservation.

$$\left(\frac{C}{N}\right)_{\text{sample}} = \left(\frac{C}{N}\right)_t \cdot f_t + \left(\frac{C}{N}\right)_m \cdot f_m, \quad (6)$$

$$f_t + f_m = 1, \quad (7)$$

where  $f_t$  and  $f_m$  are the terrestrial and marine OM fractions, respectively;  $(C/N)_t$  and  $(C/N)_m$  are the terrestrial and marine end-member values of C/N, respectively; and  $(C/N)_{\text{sample}}$  is the value of the proxy analyzed in the sediment sample. From the above equations, the following equation can be derived:

$$f_m = \frac{20 - \left(\frac{C}{N}\right)_{\text{sample}}}{15}. \quad (8)$$

### 2.6 Carbon burial fluxes

The carbon burial flux was calculated by measuring the carbon content, sedimentation rate, and dry density of sediment, based on the following equations (Ingall and Jahnke, 1994):

$$\text{BF} = C_i \times S \times \rho_d, \quad (9)$$

$$\rho_d = (1 - \phi) / ((1 - \phi) / \rho_s + \phi / \rho_w), \quad (10)$$

where BF ( $\text{g}/(\text{m}^2 \cdot \text{a})$ ) is the carbon burial flux;  $C_i$  (%) is the carbon content;  $S$  ( $\text{cm}/\text{a}$ ) is the sedimentation rate;  $\rho_d$  ( $\text{g}/\text{cm}^3$ ) is the dry density of sediment;  $\phi$  (%) is the water content in sediment;  $\rho_s$  ( $\text{g}/\text{cm}^3$ ) is the sediment grain density;  $\rho_w$  ( $\text{g}/\text{cm}^3$ ) is the density of water and  $\rho_s = 2.56 \text{ g}/\text{cm}^3$ ,  $\rho_w = 1.027 \text{ g}/\text{cm}^3$  (Dai et al., 2007).

## 3 Results

### 3.1 Chronology of the sediment cores

Based on the vertical distribution of  $^{210}\text{Pb}$  (Fig. 2), surficial

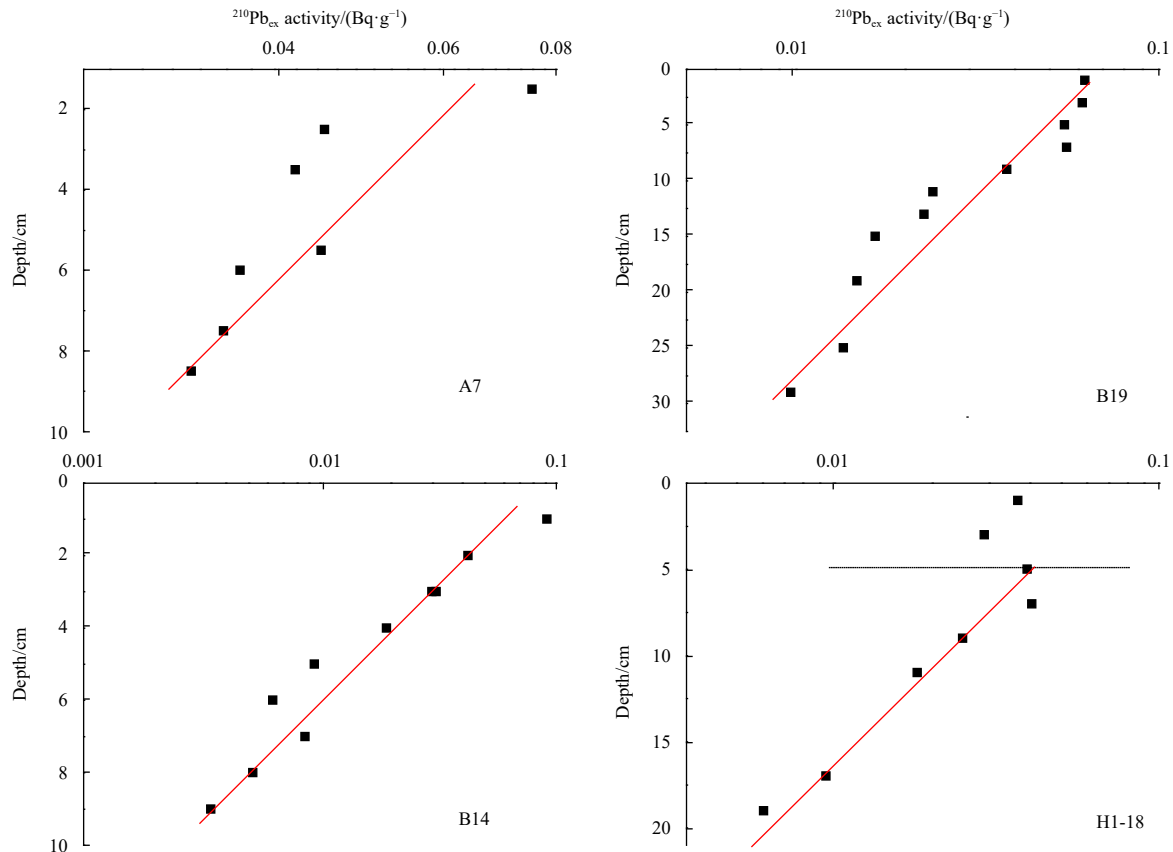
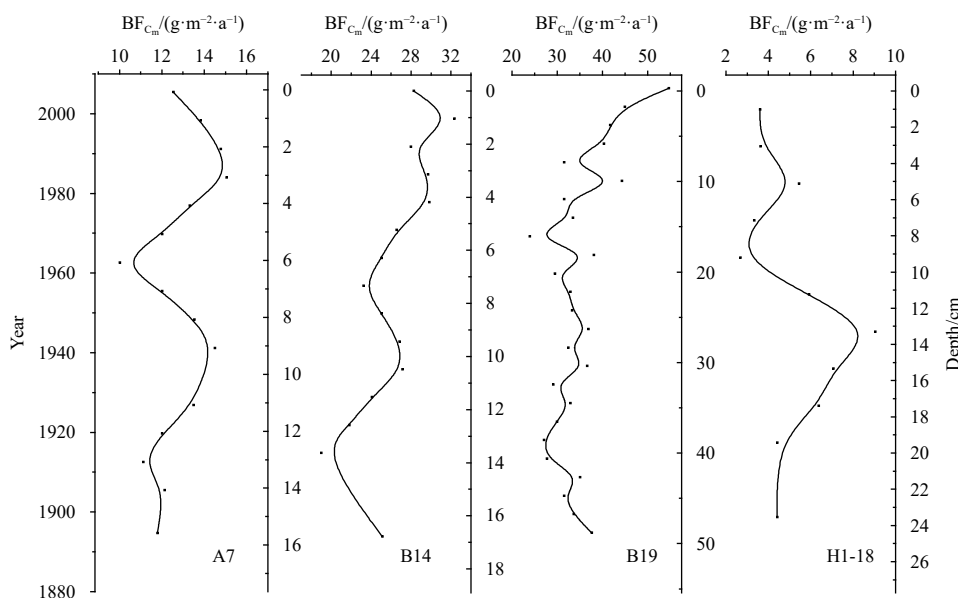


Fig. 2. Vertical distribution of  $^{210}\text{Pb}$  activities in sediment cores (squares indicate excess  $^{210}\text{Pb}$  ( $^{210}\text{Pb}_{\text{ex}}$ ) activities).

**Table 1.** Sedimentation rate, total nitrogen content (TN), total organic carbon (TOC), the ratio of carbon content vs. nitrogen content (C/N), and marine-derived organic carbon content ( $C_m$ ) in cores

Station	Water depth/m	Sedimentation rate/( $\text{cm}\cdot\text{a}^{-1}$ )	TN		TOC		C/N		$C_m$	
			Range/%	Average/%	Range/%	Average/%	Range	Average	Range/%	Average/%
A7	87	0.14	0.050–0.075	0.064	0.37–0.55	0.46	6.66–7.68	7.23	0.21–0.33	0.28
B14	80	0.15	0.124–0.171	0.140	1.05–1.52	1.28	8.06–11.34	9.19	0.37–0.63	0.51
B19	43	0.44	0.039–0.091	0.057	0.36–0.66	0.43	6.27–9.42	7.52	0.14–0.39	0.26
H1-18	63	0.22	0.038–0.050	0.043	0.56–0.79	0.67	12.57–17.56	15.41	0.04–0.12	0.07

**Fig. 3.** The interdecadal distribution of the buried flux of marine organic carbon ( $BF_{C_m}$ ) in cores.

mixing layers are observed in Core H1-18 but not in Cores A7, B19, and B14. Sedimentation rates are estimated based on a logarithmic decreasing trend of  $^{210}\text{Pb}_{\text{ex}}$  with depth (Table 1). Notably, the calculated values were consistent with the sedimentation rates reported by Yang et al. (2012). The sedimentation rate of A7, B14, B19 and H1-18 were 0.14 cm/a, 0.15 cm/a, 0.44 cm/a and 0.22 cm/a, respectively (Fig. 3). Based on these sedimentation rates and the length of the core, the sedimentation in these cores can be dated back 100 a.

### 3.2 TN, TOC, C/N and $C_m$ in cores

The values of TN, TOC, C/N, and  $C_m$  in these cores are listed in Table 1. As shown in Table 1, TN contents range from 0.038% to 0.171%, TOC contents range from 0.36% to 1.52%, C/N values range from 6.27 to 17.56,  $C_m$  range from 0.04% to 0.63% in these four cores, which are similar to previous results in the surrounding areas (Hu et al., 2016; Song et al., 2018).

### 3.3 $BF_{C_m}$ in sediment cores

The vertical distribution of  $BF_{C_m}$  in cores is shown in Fig. 3. From these data, it may be seen that  $BF_{C_m}$  in Core A7 exhibited a slight upward trend from bottom to surface, with 2.5 cycles over the past 100 a. The peak value of  $BF_{C_m}$  in Core A7 was observed in 1941 and 1984, and the valley value appeared in 1912, 1963 and 2004.

The  $BF_{C_m}$  in Core B14 also showed a slight upward trend from the bottom layer to the surface layer. In the past 100 a, there were some obvious alternations of peaks and valleys, with peaks appearing in 1936, 1978, 1985, and 1999, and valleys appearing in 1915, 1951, 1991 and 2004.

The values of  $BF_{C_m}$  in Core B19 were relatively constant (27.08–37.59  $\text{g}/(\text{m}^2\cdot\text{a})$ ) from the bottom to 20 cm depth (about the 1960s). After the 1960s, the value of  $BF_{C_m}$  fluctuated significantly, especially after 1988, when it rose rapidly and reached its peak in 2006. However, other sedimentary columns did not experience such dramatic fluctuations.

The  $BF_{C_m}$  value in Core H1-18 was relatively high and stable before 1960, and the peak appeared in 1945 at 9.04  $\text{g}/(\text{m}^2\cdot\text{a})$ . Then, the  $BF_{C_m}$  at this station continued to decline, reaching the lowest value in 1964, and remained at a relatively low level in the last years.

By comparing the interdecadal distribution of the  $BF_{C_m}$  in Cores A7 and B14, it can be concluded that the similar trends of the decadal marine-derived carbon storage of the two stations is typical of the CYSM. Thus, the reconstructed sediment records in Cores A7 and B14 are effective materials to better understand the typical characteristics of  $C_m$  storage in the CYSM. Core B19 is located to the southwest of Shandong Peninsula.  $BF_{C_m}$  in Core B19 was relatively stable before the 1960s, while the value of  $BF_{C_m}$  increased rapidly after the 1960s and reached a maximum value in the surface layer. Core H1-18 is located in the ECS. The  $BF_{C_m}$  in Core H1-18 is relatively higher before the 1960s. In more recent years, there is a declining trend and  $BF_{C_m}$  remains at a relatively lower level. The above results indicate that although the four stations are located in the ECSS, interdecadal variations in  $BF_{C_m}$  exhibit significant regional differences.

## 4 Discussion

The cores used in this study are all located in the ECSS;

however, the factors leading to regional differences in the inter-decadal variation of the  $BF_{C_m}$  remain unclear. Therefore, to better understand the possible mechanisms controlling  $BF_{C_m}$  in our study area, four sediment cores were analyzed from which to derive a preliminary understanding of the causes of regional differences.

#### 4.1 Stability of $C_m$

The stability of  $C_m$  is an important factor affecting  $C_m$  storage. The method of Tunnicliffe et al. (2001) was carried out to investigate the stability of  $C_m$ . From the data shown in Fig. 4, a significant positive correlation was observed between the  $\Sigma C_m$  and year in Cores A7, B19 and H1-18, indicating that the sedimentary  $C_m$  in these cores remained stable over the last 100 a. In contrast, the  $\Sigma C_m$  in Core B14 fluctuated significantly in the bottom layer (about the 1900s), suggesting that the state of the  $C_m$  was probably unstable. Recently the stability of  $C_m$  was also reported by Yang et al. (2012) and Yang et al. (2015). Their results showed that the depositional setting in the CYSM facilitates the preservation of sedimentary  $C_m$  over the 100 a time scale. Therefore, it is reasonable to infer that degradation is also not the main factor affecting the  $C_m$  storage in the study area (including Core B14).

#### 4.2 Sources of organic matter

Organic carbon mainly exists in the form of OM. Consequently, studies on the origins of OM can reflect potential sources of organic carbon. Studies on the sources of sedimentary OM in the ECSS play an important role in exploring the problem of the regional differences of organic carbon buried flux in these sea areas.

As shown in Fig. 5, the  $f_m$  in Core B19 ranged from 77.41% to 91.53%, with a mean value of  $83.36\% \pm 3.24\%$ . In Core A7, the  $f_m$  ranged from 82.13% to 88.95%, with a mean value of  $85.10\% \pm 1.94\%$ . In Core B14, the  $f_m$  ranged from 57.74% to 79.59%, with a mean value of  $72.06\% \pm 5.78\%$ . In Core H1-18, the  $f_m$  varied from 16.29% to 49.56%, with a mean value of  $30.58\% \pm 9.75\%$ . Compared with Core H1-18, Cores B19, A7, and B14 had higher  $f_m$ . Thus, it may be concluded that Core H1-18 is mainly affected by terrigenous source input, but that Cores B19, A7 and B14 are

mainly controlled by marine source input. The results indicate that the regional differences in the sources of OM in ECSS play an important role in controlling regional differences in organic carbon burial flux.

#### 4.3 Primary productivity versus burial flux

Decadal-scale variations in primary productivity cannot be directly studied because of the lack of long-term field investigation data in China. However, the historical records of primary productivity can be reconstructed from the contents of Biological silicon (BSi) in sediment cores (Jiang et al., 2011; Romero et al., 2015). In the ECSS, the stability of BSi and the positive correlation between the BSi and primary productivity indicate that trends in decadal primary productivities in our study areas could be largely related to decadal-scale alterations in BSi (Ye et al., 2004; Yang et al., 2012). In this study, we employed the long-term trends of BSi to qualitatively evaluate decadal-scale changes in primary productivities. The BSi data used in this study are quoted from Yang et al. (2012).

In Cores B14, A7 and B19, increased primary productivities are probably due to the increased inputs of terrestrial nutrients caused by the rapid development of agriculture and industry in China over the course of the 20th and beginning of the 21st centuries (Fig. 6). In China, chemical fertilizers were first used in 1952, and have since been widely used (Zhang, 1983). By wind, river runoff, and other means, a large number of terrigenous nutrients were transported to the offshore area, which promoted the rise of primary productivity. Increased primary productivity leads to increased burial of  $C_m$ . Thus, the increased  $BF_{C_m}$  in the Yellow Sea since the 1950s may be mainly affected by the changes in ecological environments caused by human activities. Additionally, it should be noted that the innovations of the western industrial revolution, which spread to China in roughly to 1860s, also had a promotional effect on China's economy in the late 19th century. However, the  $BF_{C_m}$ , BSi and phytoplankton biomarkers in cores did not change obviously between the late 19th century and the 1950s (Yang et al., 2012; Yang et al., 2017; Cao et al., 2017). Although China's economy developed at that time, this economic development was relatively slow and limited due to

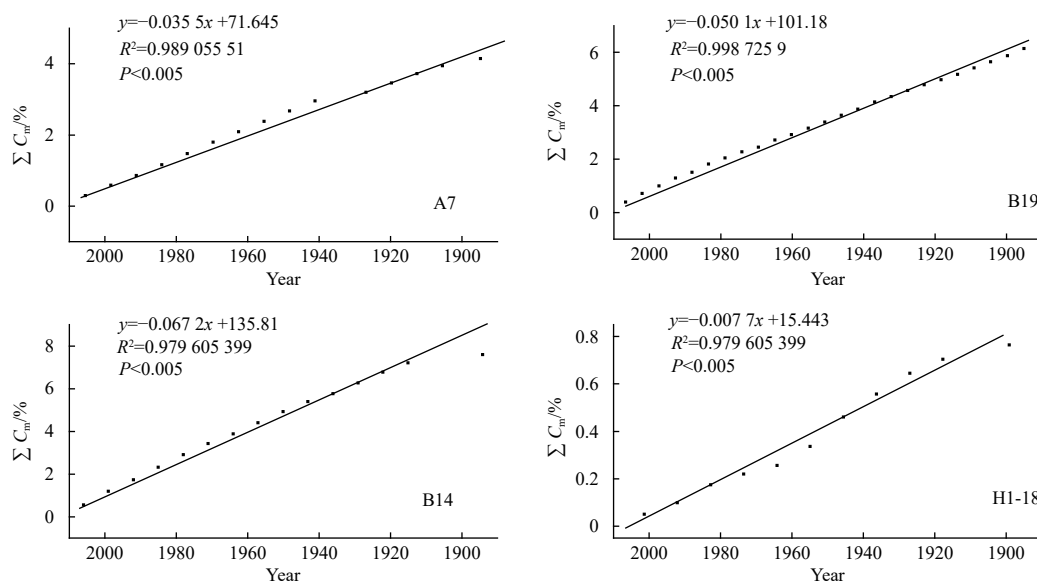
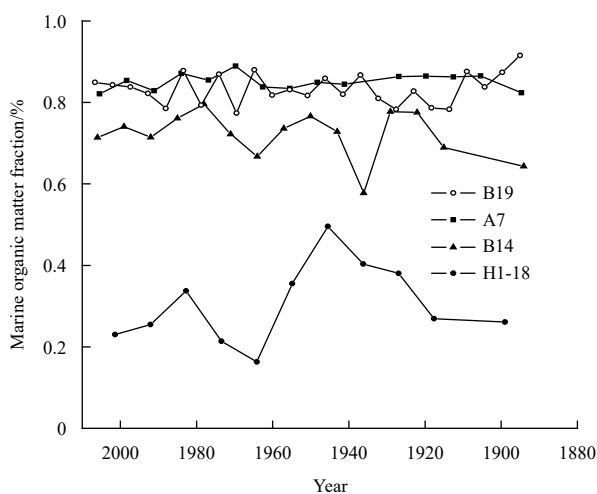


Fig. 4. Linear regression analysis of  $\Sigma C_m$  vs. year.  $C_m$ , marine-derived organic carbon content;  $\Sigma C_m$ , the sum  $C_m$  content of the increased  $C_m$  per year of all the previous years.



**Fig. 5.** Temporal variations in the marine organic matter fraction of cores.

national and international limitations. As a result, the ecologic environment in the Yellow Sea did not change obviously at that time, and the values of the  $BF_{C_m}$ , BSi and phytoplankton biomarkers in marine sediments remained relatively constant. The temporal variation of  $BF_{C_m}$  and BSi in Core H1-18 is different. This phenomenon is probably related to the disturbance of terrestrial organic matter inputs. Based on the data shown in Fig. 5, the terrestrial OM fractions ( $f_l$ ) are 1.02–5.14 times the marine OM fractions ( $f_m$ ). Given that the organic carbon contained in OM is mainly source from the land, the correspondence between  $BF_{C_m}$  and primary productivity may be different. This observation indicates that the relationship between the  $BF_{C_m}$  and primary productivities is an important factor leading to regional

differences in organic carbon burial flux.

**4.4 Pacific decadal oscillation (PDO) and EAWM versus the  $BF_{C_m}$**

Variations attributable to the PDO were determined based on the first mode of the empirical orthogonal function decomposition of abnormal monthly SST data in the North Pacific north of 20°N. We smoothed the PDO to explain the influence of PDO on changes in  $BF_{C_m}$ . Considering the extensive influence of the EAWM on the ECSS, EAWM variations are also drawn in the figure and smoothed to discuss the influence of EAWM on  $BF_{C_m}$  changes (Fig. 7).

Cores A7 and B14 are located in the CYSM.  $BF_{C_m}$  in these two cores exhibited obvious correlations between the PDO and EAWM over the past 100 a (Fig. 7). This similar phenomenon also appeared in the early studies of the CRE, the ECS and the Japan Sea (Kuwaie et al., 2006; Wang, 2014), which could be predicted through nutrient supplement analysis in these areas. Nutrients are necessary for phytoplankton growth. Nutrients in the euphotic layer of the open sea are mostly supplied from deeper water by vertical mixing (Tian et al., 2003). Figure 7 shows that the PDO index is positive, and that the EAWM index is also higher. A stronger EAWM leads to stronger winter winds derived from the north, enhancing the YSCC. As a compensation for the YSCC, upwelling associated with the YSWC increases, which can also enhance bottom intrusions (Wang and Yu, 2014). Hence, more nutrients from deeper water are transported to the euphotic layer and consumed by phytoplankton for their growth (Tan and Shi, 2012). In contrast, when the PDO is negative, the EAWM index is also lower. Limited bottom intrusions can reduce the transportation of nutrients from deeper water to upper water and limit the growth of phytoplankton and the  $BF_{C_m}$ .

Core B19 is located near the 50 m isobath southwest of Shandong Peninsula. Before the 1950s, the trends of EAWM and  $BF_{C_m}$  in this core are similar (Fig. 6). When the EAWM increases, strong

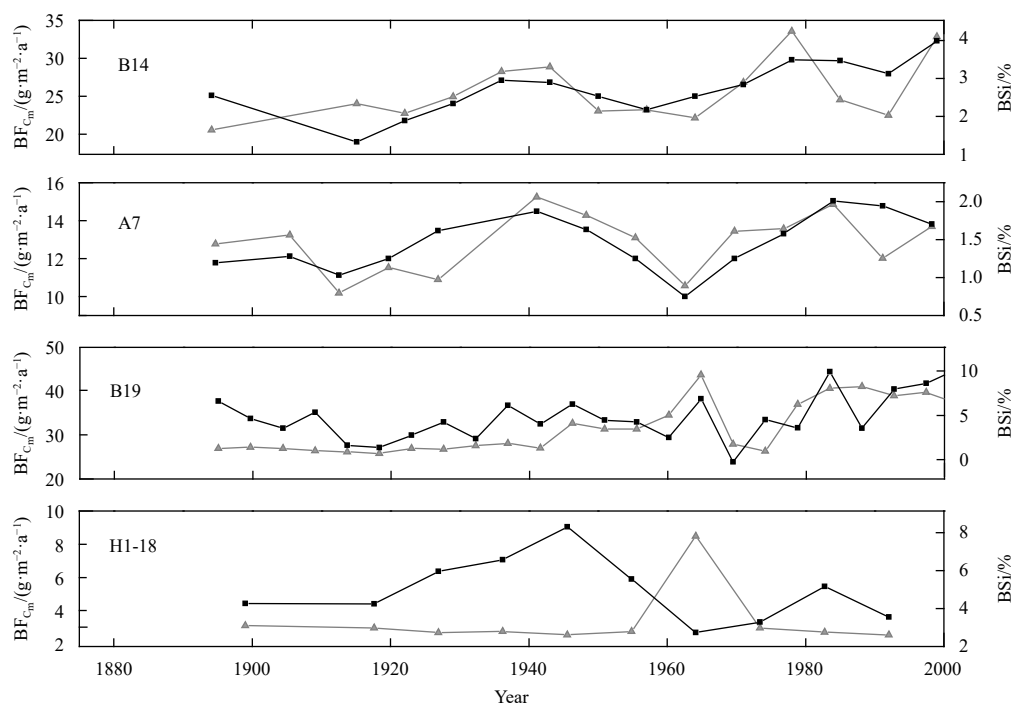


**Fig. 6.** Temporal variations in the buried flux of marine organic carbon ( $BF_{C_m}$ ) and biological silicon (BSi). The triangle represents BSi, and the square represents  $BF_{C_m}$ . BSi data are quoted from Yang et al. (2012).

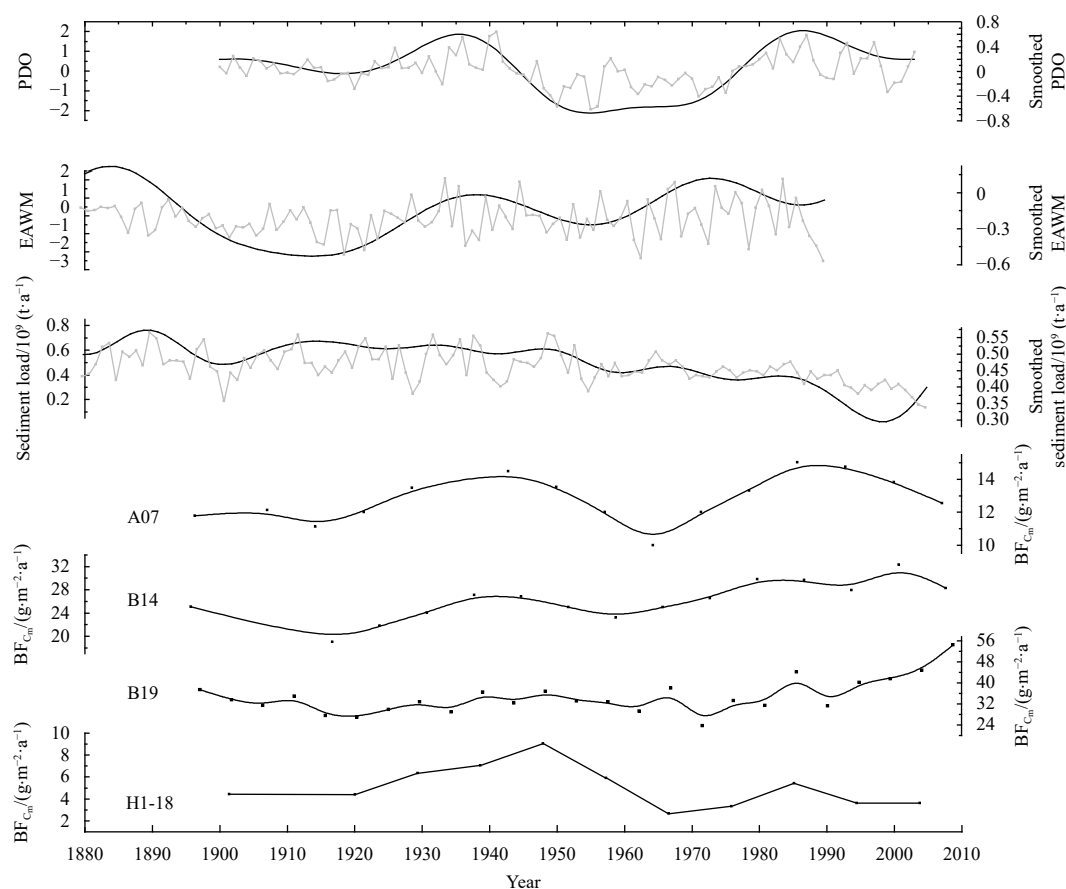


Fig. 7. Decadal changes of the buried flux of marine organic carbon ( $BF_{C_m}$ ), Pacific decadal oscillation (PDO), East Asian winter monsoon index (EAWM) and Changjiang River Estuary sediment load. Raw data of PDO, EAWM and sediment load are cited from Yang et al. (2017), Huang (2015), and Wang et al. (2008), respectively.

winter winds blow from the north, enhancing the YSCC and transport of nutrients from the Huanghe River Estuary to the location of Station B19. Thus, an enhanced EAWM can promote primary productivity in the surrounding sea area, leading to increases in  $BF_{C_m}$ . In contrast, the  $BF_{C_m}$  exhibits a decreasing trend with EAWM. After the 1950s, the  $BF_{C_m}$  at Station B19 continued to rise and remained at a higher level. Increased  $BF_{C_m}$  in Core B19 could be attributed to the enhanced inputs of terrestrial nutrients caused by China's economic development. GDP in China increased from 105.8 billion dollars in the 1970s to 2 552.9 billion dollars in the 2000s (Yang et al., 2017). In support of this conclusion, the correspondence between EAWM and  $BF_{C_m}$  also decreased during this time.

#### 4.5 Sediment load versus $BF_{C_m}$

Sediments in the SYS and ECS are primarily influenced by the supply of terrestrial sources from the Huanghe River and the Changjiang River. Cores B19 and H1-18 are close to the shore and are likely to be most affected by river input. Previous studies revealed that the nutrients in Shandong Peninsula are mainly attributable to transport of nutrients from the Huanghe River by the YSCC (Hu et al., 2016). Since the 1980s, the sediment load from the Huanghe River decreased rapidly. However, it still contributes a huge flux of sediments (up to  $1.1 \times 10^9$  t/a) to the adjacent sea. Therefore, the deposition rates of sediment in Core B19 are relatively higher (mean value of 0.44 cm/a). High sediment accumulation rates could facilitate a rapid burial of particulate

organic carbon, which in turn may reduce the exposure time of sediments to bioturbation and/or oxic decomposition, enhancing its preservation (Kuehl et al., 1993; Carroll et al., 2008). Therefore, Core B19 has the largest  $BF_{C_m}$  among the four cores. Core H1-18 ( $30.5^\circ\text{N}$ ,  $123.5^\circ\text{E}$ ) is located near the CRE (the east of the high deposition area). Because the belt at longitude  $122.5^\circ$ – $123^\circ\text{E}$  is the front where the diluted water of the Changjiang River meets the sea water on the continental shelf, flocculation is strong and the deposition rate can reach up to 6.3 cm/a (Duan et al., 2005). Flocculation of dissolved/particles in the high deposition area inhibits the eastward transportation of suspended particles in the CRE, which can decrease the transport of nutrients and total primary productivity to the sea (Shi, 2016). Thus, the conservation efficiency of  $f_m$  in sediments and the average of the  $BF_{C_m}$  in Core H1-18 is the lowest among the four stations we studied.

Because Core H1-18 is mainly affected by inputs from terrestrial sources (Fig. 5), this study suspects that the core may also be influenced by the input of organic matter and nutrients from the Changjiang River, which is consistent with the sediment load of the Changjiang River. Sediment loads are drawn in Fig. 7 to discuss the influence of sediment load on regional differences in  $BF_{C_m}$ .

From the data shown in Fig. 7, it can be seen that the  $BF_{C_m}$  in H1-18 has no significant correlation with the PDO or the EAWM. However, the variation of the  $BF_{C_m}$  is similar to the input of sediment load from the Changjiang River during the past 100 a. This

similar phenomenon also appears in the investigation and analysis of biomarkers in the CRE (Cao et al., 2017). Human activities dominated the transport of large sediment loads ( $0.5 \times 10^9$  t/a) from the Changjiang River Basin to the sea between 1900 and 1950. Sediment load decreased from  $0.5 \times 10^9$  t/a (1950–1960) to  $0.33 \times 10^9$  t/a (1970–1990) due mainly to the construction of dams along the river. This reduction in sediment load means the organic matter and nutrients from the Changjiang River was reduced and primary production was also reduced, leading to a reduction in  $BF_{C_m}$ .

## 5 Conclusions

This study concludes that decadal-scale variations in  $BF_{C_m}$  in the studied cores are affected by numerous factors including the organic matter sources, primary productivity, sediment accumulation rates, sediment load, PDO and EAWM. However, human activities and differences in marine environments are key factors controlling regional differences and decadal changes of the  $BF_{C_m}$ . Before the 1950s, the burial of  $BF_{C_m}$  in the ECSS was mainly controlled by the marine environment under natural conditions. After 1950,  $BF_{C_m}$  in the CYSM remained under the influence of natural conditions and exhibits periodic changes. In contrast,  $BF_{C_m}$  in the YSCC and the CRE exhibit trends that suggest  $BF_{C_m}$  in these regions is now primarily controlled by human activities. Taken together, these results suggest that decadal changes in  $BF_{C_m}$  are characterized by regional variations in a complex ocean environment. To gain a better understanding of the long term changes of  $BF_{C_m}$  on the continental shelf and the related mechanisms of  $C_m$  sequestration, future research should focus on the relationship between the  $BF_{C_m}$  and long term environmental changes in the complex shelf environment.

## Acknowledgements

We thank two anonymous reviewers for their constructive comments. We also thank Xin Zhou for his enthusiastic encouragement and help.

## References

- Cai Deling, Sun Yao, Zhang Xiaoyong, et al. 2014. Reconstructing a primary productivity history over the past 200a using the sediment organic carbon content and the stable isotope composition from the East China Sea and the Yellow Sea. *Haiyang Xuebao* (in Chinese), 36(2): 40–50
- Cao Yunyun, Xing Lei, Zhang Ting, et al. 2017. Multi-proxy evidence for decreased terrestrial contribution to sedimentary organic matter in coastal areas of the East China Sea during the past 100 years. *Science of the Total Environment*, 599–600: 1895–1902
- Carroll J, Zaborska A, Papucci C, et al. 2008. Accumulation of organic carbon in western Barents Sea sediments. *Deep-Sea Research Part II: Topical Studies in Oceanography*, 55(20–21): 2361–2371
- Chen Bin, Hu Limin, Deng Shenggui, et al. 2011. Organic carbon in surface sediments of the Bohai Bay, China and its contribution to sedimentation. *Marine Geology & Quaternary Geology* (in Chinese), 31(5): 37–42
- Dai Jicui, Song Jinming, Li Xuegang, et al. 2007. Geochemical characteristics of nitrogen and their environmental significance in Jiaozhou Bay sediments. *Quaternary Sciences* (in Chinese), 27(3): 347–356
- Dean W E. 1999. The carbon cycle and biogeochemical dynamics in lake sediments. *Journal of Paleolimnology*, 21(4): 375–393, doi: 10.1023/A:1008066118210
- Duan Lingyun, Wang Zhanghua, Li Maotian, et al. 2005.  $^{210}\text{Pb}$  distribution of the Changjiang estuarine sediment and the implications to sedimentary environment. *Acta Sedimentologica Sinica* (in Chinese), 23(3): 514–522
- Hu Limin, Shi Xuefa, Bai Yazhi, et al. 2016. Recent organic carbon sequestration in the shelf sediments of the Bohai Sea and Yellow Sea, China. *Journal of Marine Systems*, 155: 50–58, doi: 10.1016/j.jmarsys.2015.10.018
- Huang Jiansheng. 2015. Sedimentary record of anchovy population dynamics in the Yellow Sea and its response to climate change (in Chinese) [dissertation]. Xiamen: Xiamen University
- Ingall E, Jahnke R. 1994. Evidence for enhanced phosphorus regeneration from marine sediments overlain by oxygen depleted waters. *Geochimica et Cosmochimica Acta*, 58(11): 2571–2575, doi: 10.1016/0016-7037(94)90033-7
- Jia Guodong, Peng Ping'an, Fu Jiamo. 2002. Sedimentary records of accelerated eutrophication for the last 100 years at the Pearl River estuary. *Quaternary Sciences* (in Chinese), 22(2): 158–165
- Jiang Shan, Liu Xiaodong, Xu Liqiang, et al. 2011. Potential application of biogenic silica as an indicator of paleo-primary productivity in East Antarctic lakes. *Advances in Polar Science*, 22(3): 131–142
- Kuehl S A, Fuglseth T J, Thunell R C. 1993. Sediment mixing and accumulation rates in the Sulu and South China Seas: Implications for organic carbon preservation in deep-sea environments. *Marine Geology*, 111(1–2): 15–35
- Kuwae M, Yamashita A, Hayami Y, et al. 2006. Sedimentary records of multidecadal-scale variability of diatom productivity in the Bungo Channel, Japan, associated with the Pacific Decadal Oscillation. *Journal of Oceanography*, 62(5): 657–666, doi: 10.1007/s10872-006-0084-0
- Li Junlong, Zheng Binghui, Hu Xupeng, et al. 2015. Terrestrial input and nutrient change reflected by sediment records of the Changjiang River Estuary in recent 80 years. *Acta Oceanologica Sinica*, 34(2): 27–35, doi: 10.1007/s13131-015-0617-8
- Li Xuegang, Yuan Huamao, Li Ning, et al. 2008. Organic carbon source and burial during the past one hundred years in Jiaozhou Bay, North China. *Journal of Environmental Sciences*, 20(5): 551–557, doi: 10.1016/S1001-0742(08)62093-8
- Lin Tian, Wang Lifang, Chen Yingjun, et al. 2014. Sources and preservation of sedimentary organic matter in the Southern Bohai Sea and the Yellow Sea: Evidence from lipid biomarkers. *Marine Pollution Bulletin*, 86(1–2): 210–218
- Meyers P A. 1994. Preservation of elemental and isotopic source identification of sedimentary organic matter. *Chemical Geology*, 114(3–4): 289–302
- Perdue E M, Koprivnjak J F. 2007. Using the C/N ratio to estimate terrigenous inputs of organic matter to aquatic environments. *Estuarine, Coastal and Shelf Science*, 73(1–2): 65–72
- Qian Junlong, Wang Sumin, Xue Bin, et al. 1997. A method of quantitative estimating terrestrial organic carbon in lake sedimentation research. *Chinese Science Bulletin* (in Chinese), 42(15): 1655–1657
- Romero O E, Kim J H, Bárcena M A, et al. 2015. High-latitude forcing of diatom productivity in the southern Agulhas Plateau during the past 350 kyr. *Paleoceanography*, 30(2): 118–132, doi: 10.1002/2014PA002636
- Shi Qiang. 2016. Climate response and spatio-temporal modes on the interannual summer changes of temperature-salinity in North Yellow Sea. *Journal of Applied Oceanography* (in Chinese), 35(4): 469–483
- Song Jinming, Qu Baoxiao, Li Xuegang, et al. 2018. Carbon sinks/sources in the Yellow and East China Seas—Air-sea interface exchange, dissolution in seawater, and burial in sediments. *Science China Earth Sciences*, 61(11): 1583–1593, doi: 10.1007/s11430-017-9213-6
- Tan Saichun, Shi Guangyu. 2012. The relationship between satellite-derived primary production and vertical mixing and atmospheric inputs in the Yellow Sea cold water mass. *Continental Shelf Research*, 48: 138–145, doi: 10.1016/j.csr.2012.07.015
- Tian Tian, Wei Hao, Su Jian, et al. 2003. Study on cycle and budgets of nutrients in the Yellow Sea. *Advances in Marine Science* (in Chinese), 21(1): 1–11
- Tunnicliffe V, O'Connell J M, McQuoid M R. 2001. A Holocene record of marine remains from the Northeastern Pacific. *Marine Geology*, 174: 197–210, doi: 10.1016/S0025-3227(00)00150-X



- Wang Liang. 2014. High-resolution sedimentary record in the typical mud areas of East China Sea and its response to climate and environmental changes (in Chinese) [dissertation]. Qingdao: Ocean University of China
- Wang Ran, Yu Fei. 2014. Impact of climatic change on sea surface temperature variation in Subei coastal waters, East China. *Chinese Journal of Oceanology and Limnology*, 32(6): 1406–1413, doi: 10.1007/s00343-015-3336-2
- Wang Houjie, Yang Zuosheng, Wang Yan, et al. 2008. Reconstruction of sediment flux from the Changjiang (Yangtze River) to the sea since the 1860s. *Journal of Hydrology*, 349(3–4): 318–332
- Wu Peng, Bi Rong, Duan Shanshan, et al. 2016. Spatiotemporal variations of phytoplankton in the East China Sea and the Yellow Sea revealed by lipid biomarkers. *Journal of Geophysical Research: Biogeosciences*, 121(1): 109–125, doi: 10.1002/2015JG003167
- Yang Qian, Song Xianli, Sun Yao, et al. 2012. Application of biogenic silicon in modern sedimentary section to reconstruction of phytoplankton changes in the East China Sea and the Huanghai Sea during last 200 years. *Acta Oceanologica Sinica*, 31(2): 70–77, doi: 10.1007/s13131-012-0193-0
- Yang Shouye, Tang Min, Yin W W S, et al. 2011. Burial of organic carbon in Holocene sediments of the Zhujiang (Pearl River) and Changjiang (Yangtze River) estuaries. *Marine Chemistry*, 123(1–4): 1–10
- Yang Shu, Yang Qian, Liu Sai, et al. 2015. Burial fluxes and sources of organic carbon in sediments of the central Yellow Sea mud area over the past 200 years. *Acta Oceanologica Sinica*, 34(10): 13–22, doi: 10.1007/s13131-015-0723-7
- Yang Shu, Yang Qian, Qu Keming, et al. 2017. Regional differences in decadal changes of diatom primary productivity in the eastern Chinese shelf sea over the past 100 years. *Quaternary International*, 441: 140–146, doi: 10.1016/j.quaint.2016.07.034
- Ye Xiwen, Liu Sumei, Zhao Yingfei, et al. 2004. The distribution of biogenic silica in the sediments of the East China Sea and the Yellow Sea and its environmental signification. *China Environmental Science (in Chinese)*, 24(3): 265–269
- Zhang Tong. 1983. Correlation analysis between fertilizer use and food production. *Journal of Agrotechnical Economics (in Chinese)*, (5): 11–14
- Zhang Yao, Zhao Meixun, Cui Qiu, et al. 2017. Processes of coastal ecosystem carbon sequestration and approaches for increasing carbon sink. *Science China Earth Sciences*, 60(5): 809–820, doi: 10.1007/s11430-016-9010-9